JOURNAL OF NEUROTRAUMA
Volume 23, Number 8, 2006

Pp. 1222–1232

Material Properties of Human Infant Skull and Suture at High Rates

BRITTANY COATS and SUSAN S. MARGULIES

ABSTRACT

Clinicians are often faced with the challenging task of distinguishing between accidental and inflicted pediatric head trauma. There is currently a disparity in the anecdotal case study literature as to what kinds of injuries can occur in children from low height falls. There is also a paucity of material property data for pediatric skull and suture at rates similar to those expected in low height falls. We tested human infant (<1 year old) cranial bone and suture from 23 calveria in three-point bending and tension, respectively, at rates ranging from 1.2–2.8 m/sec. Donor age was found to have the largest influence on the elastic modulus and ultimate stress of cranial bone, with an increase in age increasing both material properties. In adults, cranial bone and suture have similar properties and the adult calveria deforms very little prior to fracture. In contrast, pediatric cranial bone is 35 times stiffer than pediatric cranial suture. In addition, pediatric cranial suture deforms 30 times more before failure than pediatric cranial bone and 243 times more than adult cranial bone. The large strains in the pediatric bone and suture result in a skullcase that can undergo dramatic shape changes before fracture, potentially causing substantial deformation in the brain. The sizeable difference between pediatric bone and suture material properties also underscores the crucial role that sutures play in the unique response of the pediatric head to impact in low height falls. These data provide necessary information to enhance our understanding of mechanisms of head injury in young children.

Key words: head injury; high rate; infant; material properties; skull; suture

INTRODUCTION

UNINTENTIONAL FALLS are the most common causes of severe head injury to young children (Langlois et al., 2004). Clinicians are often faced with the challenge of distinguishing between accidental and inflicted trauma when presented with an injured child. This proves to be a difficult task given that falls are the most common excuse provided by caretakers suspected of child abuse (Lane et al., 2002) and that there is a disparity in the literature regarding the types of injuries that can be produced by falls from various heights (Chadwick et al., 1991; Tarantino et al., 1999; Weber, 1984, 1985; Williams, 1991).

The possible types of injuries resulting from low height falls are more likely to be identified if the dynamic material properties of pediatric suture and skull are known. Material properties such as elastic modulus, ultimate stress, and ultimate strain dictate the response and failure of a material to loading. The elastic modulus is an

Department of Bioengineering, University of Pennsylvania, Philadelphia, Pennsylvania.

indication of the stiffness, or resistance to deformation, of a material. The ultimate stress and strain are indications of the maximum force and deformation, respectively, that a material can undergo before it fails. Determining the material properties of pediatric skull and suture will not only provide insight into the reaction of the pediatric cranial cavity to loading, but will also improve the accuracy of computational and experimental models simulating falls or impacts to a pediatric head.

There has been extensive characterization of the dynamic material properties of adult skull tissue (McElhaney et al., 1970; Wood, 1971), but dynamic properties of pediatric skull and suture remain relatively unknown. McPherson and Kriewall (1980a) were the first to investigate pediatric skull material related to fetal head molding. They performed three-point bending tests at quasi-static rates of 8.33×10^{-6} m/sec (0.5 mm/min) on multiple parietal and frontal skull specimens from six fetal calvaria (26–40 weeks gestation). Specimens were tested with the grain fibers running parallel to the long axis of the specimen and others were tested with the grain fibers running perpendicular to the long axis of the specimen. McPherson and Kriewall found significant difference between the elastic moduli of the parallel and perpendicular oriented specimens and concluded that there was an anisotropic, or directional, effect on the material properties. Moduli of preterm (24–30 weeks gestation) specimens were also found to be significantly lower than moduli of term (36–40 weeks gestation) specimens, regardless of fiber orientation. More recently, Margulies and Thibault (2000) examined multiple specimens from four human pediatric calveria (28 weeks gestation to 6 months) in three-point bending at rates of 4.23×10^{-5} m/sec (2.54 mm/min) and 4.23×10^{-2} m/sec (2540 mm/min), typical of a slow "crush" event. They found donor age had a significant effect on the elastic modulus of pediatric skull. In addition, they reported that pediatric skull elastic modulus was 12 times lower than that of adult cortical compact bone from the outer table of the skull.

Large rate dependence has been reported for adult skull tissue (Wood, 1971), but previous pediatric skull studies did not investigate rate dependence due to a limited number of samples. We hypothesize that there is a rate-dependence in pediatric skull as well, which would imply that the published data for the pediatric skull studies tested at slow "crush" rates (Margulies and Thibault, 2000; McPherson and Kriewall, 1980a) may not be suitable for understanding skull response to low height falls or inflicted impacts which impose deflection at rates of 2.4 m/sec or higher. Thus, in order to determine injury risk and develop effective injury interventions for infants during falls and inflicted impacts, it is important to obtain pediatric material properties at relevant rates.

The immature skull is composed of thin plates of compact bone joined by membranous suture and fontinelles. During post-natal development, the sutures fuse, fontinelles close, and the bone calcifies, thickens, and separates into compact outer and inner tables, separated by a spongy diploe layer. No data currently exist in the literature regarding the material properties of immature cranial suture or the skull-suture-skull complex. These data are crucial to developing an accurate computational model that is specific to pediatric head injury. Our goal is to define the material properties of human infant ($\leq$1 year old) skull and suture at high rates and from two cranial regions to be used in future computational models simulating the infant head during accidental and inflicted impacts. We hypothesize that bone will be significantly stiffer than suture and that suture will experience a significantly higher strain before failure than cranial bone. We further hypothesize that age of the donor and deformation rate will significantly *increase* elastic modulus and ultimate stress, and significantly *decrease* ultimate strain of pediatric cranial bone and suture. Finally, we hypothesize that the material properties of parietal cranial bone will not be significantly different than those of occipital cranial bone.

METHODS

Testing Device Validation

A drop test apparatus was designed to test samples in three-point bending and tension at high rates. The drop test apparatus and experimental design were validated by comparing measured material properties of copolymer (three-point bending) and porcine cranial suture (tension) from the drop test apparatus to measured material properties of the same materials in tension in an Instron 8501 commercial material testing device (Instron, Norwood, MA).

Human Pediatric Cranial Skull and Suture Sample Collection and Preparation

Human pediatric cranial bone and suture were collected at autopsy in a protocol approved by the University of Pennsylvania and the Children's Hospital of Philadelphia IRBs. Subjects ranged in age from preterm (21 weeks gestation) to 1 year of age. Subjects with a history of skull fracture or skull malformations were excluded from the study. Two cranial specimens were removed and frozen from each subject: one occipital bone and one parietal parasagittal sample containing suture and bone (Fig. 1).

On the day of testing, frozen cranial samples were thawed to room temperature (25°C) in a mock CSF so-

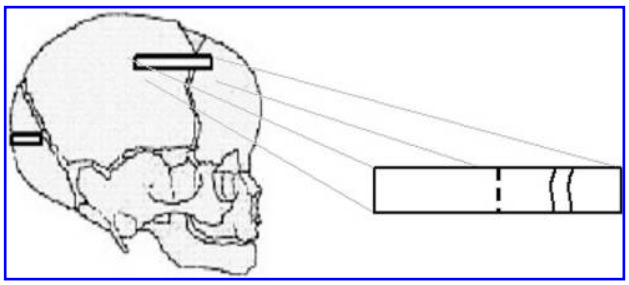

FIG. 1. Schematic indicating the locations for removal of pediatric cranial bone and suture specimens. One bone specimen was removed from the occiput of the skull, and one longer specimen containing cranial bone and coronal suture was removed from the parietal region. The longer specimen was cut in half (dotted line) to produce a parietal bone and a bone-suture-bone specimen.

lution. Using a diamond cutting blade (Stoelting Co., Wood Dale, IL) and rotary tool (Dremel®, Racine, WI), human parasagittal suture/bone specimens were cut to produce two specimens (one parietal bone, one bone-suture-bone segment). Size of the specimen depended on the tissue provided. Care was taken to ensure a uniform sample thickness for three-point bending testing. Thickness (d), width (w), and suture span (L) (when applicable) were measured. If a specimen had a unique dimension (i.e., slightly larger width or a smaller thickness near one end of the sample), this dimension was also measured and used in calculations if failure occurred in this region. Samples were tested within 1 h after completion of machining.

Material Testing

Human pediatric cranial bone samples ($N = 46$ specimens from 21 infant calveria) were tested in three-point bending using the drop test apparatus. No standard exists for performing three-point bending tests on human skull at high rates; therefore, we used ASME standard D70 to guide our specimen dimensions. Specifically, we used a minimum span length (L) to thickness ratio of 14:1, and the ASME D70 equation to calculate strain. All specimens were tested with grain fibers perpendicular to the long axis of the specimen (Fig. 2A).

Human pediatric cranial bone-suture-bone specimens ($n = 14$ specimens from 11 calveria) were tested in tension in the drop test apparatus. For all tests, the bone portion of the bone-suture-bone complex was mounted into ridged grips made of Delrin®. The gage length (L_o) was measured as the span of the suture between the bone segments (Fig. 2B).

Displacement (δ) for both three-point bending and tensile tests was measured using a laser displacement sensor

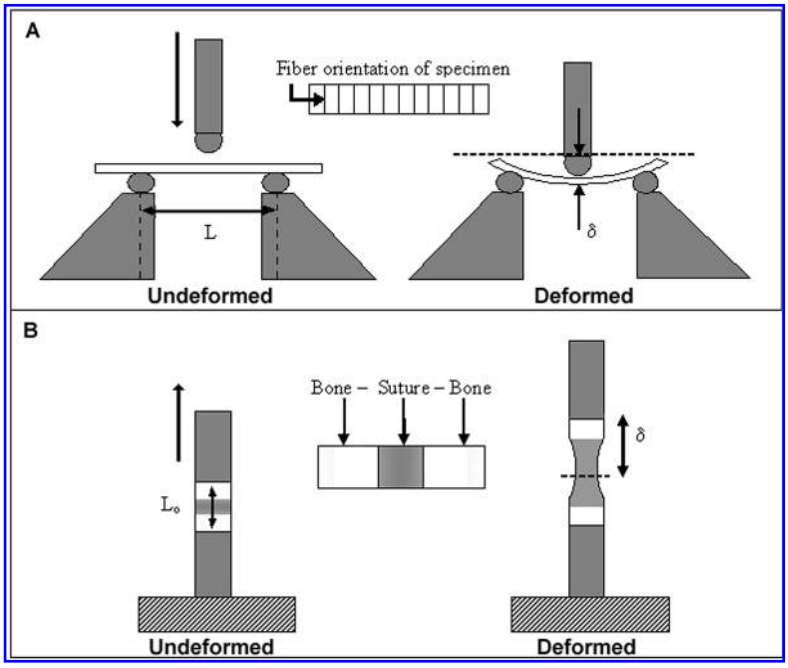

FIG. 2. Schematic of the test setup for three-point bending of human infant cranial bone (**A**) and tensile testing of human infant cranial suture (**B**). Each test yields force, F, and displacement, δ, measurements, which are used in Equations (1–5), to determine the stress and strain for each material.

(OptoNCDT 160-00, Micro-Epsilon, Ortenburg, Germany). Displacement of specimen was assumed to be equal to that of the upper knife (three-point bending) or upper grip (tension) after ensuring that no slipping occurred during testing. Force (F) was measured using a 25-lb (tension) or 50-lb (three-point bending) load cell (Sensotec, Columbus, OH). All data were collected using a computer data acquisition system (Labview 4.1, National Instruments, Austin, TX) at 10,000 samples per second, and saved onto a laptop computer (Dell, Austin, TX).

The Law of Conservation of Energy indicates that for an object of any mass, the velocity at which it hits the ground is equal to the square root of two times the gravity times the initial height of the object ($V = \sqrt{2gh}$). Applying this law to an object falling from 0.305 and 0.914 m (1 and 3 feet, respectively) would result in an ideal velocity of 2.41 and 4.23 m/sec. Test rate for this study was determined by adjusting the height of the free fall crosshead plate to 0.305 m and 0.914 m which resulted in average test rates of 1.58 and 2.81 m/sec for three-point bending tests. These values are lower than the ideal velocities calculated above because of air friction and friction caused by the guide rails of the crosshead plate. The tensile device had shock absorbent foam on the device to reduce vibration during testing. This foam absorbed part of the kinetic energy and resulted in the lower test rates of 1.20 and 2.38 m/sec for tension tests.

Data Analysis

Three-point bending. Because the span length to thickness ratio was at least 14:1, the depth of cranial bone tested in three-point bending can be assumed small and the Bernoulli-Euler equation can be applied to calculate elastic modulus (E):

$$E = \left(\frac{F}{\delta}\right)\frac{L^3}{48I} \tag{1}$$

where F/δ is the force-displacement ratio during the linear elastic region of a three-point bending trace (Fig. 3), L is the span of the beam, and I is the moment of inertia of the rectangular cross section of the beam (Timoshenko and Goodier, 1970).

In-plane stress (σ_{xx}) was calculated using Timoshenko's corrected version of the beam theory equation which accounts for radial tensile forces within the beam as a result of an applied concentrated load to the center of the beam.

$$\sigma_{xx} = \frac{3FL}{8wc^3}\, y - 0.133\,\frac{F}{wc} \tag{2}$$

where F is the measured force, w is the width of the specimen, L is the span, c is half of the thickness, and y is the location of interest along the y-axis (outer surfaces at $y = \pm c$) in the center of the beam. The ultimate stress (σ_{ult}) is then calculated by using the maximum force (F_{peak} in Fig. 3) for F in Equation (2).

The flexural strain (ε_f) from three-point bending was calculated from the relationship:

$$\varepsilon_f = \frac{6t\delta}{L^2} \tag{3}$$

where δ is the maximum deflection in the center of the beam, t is the thickness of the sample, and L is the span (ASTM D790). Ultimate strain (ε_{ult}) was selected as the flexural strain corresponding to the ultimate stress.

Tensile tests. For the tensile tests, stress was calculated using the equation for normal stress under axial loading shown in Equation (4).

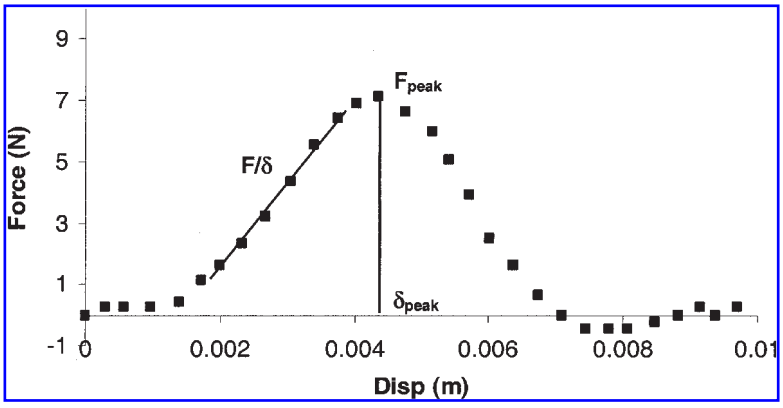

FIG. 3. Force-displacement trace from three-point bending test for parietal bone of a 2-month-old donor. The diagonal line indicates the force displacement data used to calculate bending modulus; F_{peak} and δ_{peak} indicate the peak force and displacement used to calculate ultimate stress and strain.

$$\sigma = \frac{F}{wt} \tag{4}$$

where F is the measured force, w is the width, and t is the thickness of the bone-suture-bone specimen. Because bone is an order of magnitude stiffer than suture, the measured displacement, δ, of the bone-suture-bone specimen can be attributed to the deformation of the suture rather than the bone. Engineering strain of the suture was therefore calculated as the measured displacement, δ, divided by the original span, L_o of the suture between the bone segments, as shown in Equation (5).

$$\varepsilon = \frac{\delta}{L_o} \tag{5}$$

The material properties (E, σ_{ult}, and ε_{ult}) were obtained from the stress-strain relationship as illustrated in Figure 4.

Statistical Analysis

In the case where multiple specimens were tested from the same calveria, each specimen was treated as an individual data point in statistical analysis. A three-way ANOVA was used to determine significant material property difference between strain rate, location, and donor age for human cranial bone. A two-way ANOVA was used to determine significant material property differences between strain rate and donor age of human cranial suture. A Student's *t*-test with a Type I error of 5% was used to determine significant differences between cranial bone and suture.

RESULTS

Device Validation

Material properties measured in the drop test apparatus were compared with those measured in a commercial Instron material testing device using an unpaired Student's *t*-test. Ultimate strain measured in the drop test apparatus in three-point bending ($\varepsilon_{ult\text{-}3pt}$) significantly underestimated the strain measured in tension by the Instron material testing device by 66%. We speculate that the equation used to calculate strain in three-point bending may not be detailed enough to accurately predict the complex strain dynamics of bone at these rates. The ultimate strain of human immature bone measured in this study is reported, but should be considered an underestimation of the actual strain of the material. Modulus (E) and ultimate stress (σ_{ult}) measured in both tension and three-point bending and ultimate strain measured in tension ($\varepsilon_{ult\text{-}tension}$) were not significantly different between the two devices (Coats and Margulies, 2005).

Cranial Bone

All cranial bone data is presented in Table 1. A three-way ANOVA of specimen location, donor age, and strain rate found a significant influence of both location (parietal/occipital) and donor age on bending modulus ($p_{location} = 0.038$, $p_{age} = 0.014$) and ultimate stress ($p_{location} = 0.006$, $p_{age} = 0.003$). Parietal bone ultimate stress and modulus were larger than occipital bone. Ultimate stress and modulus increased with the age of the donor. Ultimate stress was significantly affected by the three-way interaction between donor age, location, and strain rate ($p = 0.016$). Ultimate strain was the only pa-

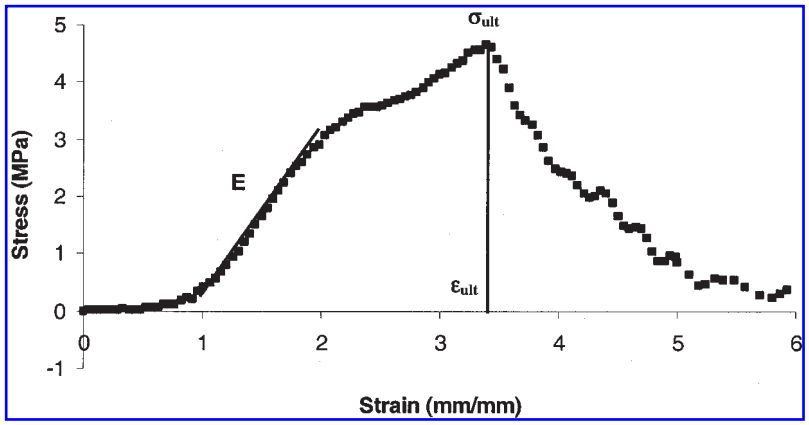

FIG. 4. Stress-strain trace of a tension test for a bone-suture-bone specimen from a 2-month-old donor. The diagonal line, E, indicates the data used to calculate elastic modulus, and σ_{ult} and ε_{ult} indicate the data points used to designate ultimate stress and strain.

Table 1. All Data Points for Parietal and Occipital Cranial Bone Tested Three-Point Bending

Cranium	*Age*	*Region*	*Bending modulus (MPa)*[a]	*Ultimate stress (MPa)*[a]	*Ultimate stress (mm/mm)*[a]
1	21 wks gest	Occipital	181.1	12.5	0.0627
2	28 wks gest	Occipital	45.3	8.8	0.0071
3	28 wks gest	Occipital	89.4	9.8	0.0027
		Occipital	132.9	12.3	0.0020
		Parietal	50.2	5.5	0.0037
		Parietal	120.1	5.6	0.0089
4	32 wks gest	Occipital	58.7	3.3	0.0416
5	34 wks gest	Parietal	552.9	81.1	0.0045
6	35 wks gest	Parietal	97.0	7.0	0.0026
7	38 wks gest	Occipital	290.0	12.6	0.0467
		Occipital	448.1	31.4	0.0735
8	39 wks gest	Occipital	211.1	6.7	0.0501
		Occipital	229.3	7.4	0.0346
		Parietal	253.9	7.6	0.0264
		Parietal	933.1	31.8	0.0431
10	19 days old	Parietal	336.8	37.8	0.1490
12	21 days old	Occipital	550.7	5.8	0.0125
		Occipital	516.2	4.6	0.0068
		Parietal	182.7	8.4	0.0450
13	1 mo old	Occipital	449.2	18.5	0.0465
		Parietal	815.5	53.7	0.0753
14	1.5 mo old	Occipital	28.6	8.7	0.0068
		Occipital	57.7	13.5	0.0039
15	1.5 mo old	Parietal	372.4	19.7	0.0700
		Parietal	518.2	29.6	0.0533
		Parietal	581.3	25.6	0.0639
16	1 mo, 23 days old	Occipital	421.4	15.1	0.0314
17	2 mo old	Parietal	297.4	14.2	0.0515
		Parietal	522.4	27.1	0.0765
18	2 mo, 9 days old	Occipital	186.4	3.1	0.0259
		Occipital	186.1	5.7	0.0268
19	3 mo old	Occipital	1317.6	43.4	0.0254
		Occipital	463.5	26.1	0.0456
		Parietal	1155.2	69.7	0.0807
20	4.5 mo old	Occipital	317.7	16.4	0.0542
		Occipital	392.8	19.5	0.0538
		Parietal	552.4	23.7	0.0500
21	11 mo old	Occipital	602.9	37.6	0.0030
		Occipital	322.1	17.3	0.0031
		Parietal	783.8	52.1	0.0032
		Parietal	573.0	48.8	0.0034
22	12 mo old	Occipital	104.2	6.2	0.0538
		Occipital	621.8	21.2	0.1613
		Parietal	200.8	19.3	0.1217
		Parietal	566.5	51.5	0.0936
23	13 mo old	Parietal	216.8	15.1	0.0885

[a]Load and displacement instrumentation accuracy is 0.02% and 1.0×10^{-4}, respectively.
Wks, weeks; gest, gestation; mo, month.

Table 2. Material Properties for Cranial Suture Specimens Tested in Tension

Cranium	*Age*	*Elastic modulus (MPa)*[a]	*Ultimate stress (MPa)*[a]	*Ultimate strain (mm/mm)*[a]
1	21 wks gest	N/A[b]	3.5	N/A
2	28 wks gest	14.2	6.7	0.6943
		13.2	6.3	4.7029
4	32 wks gest	4.3	4.5	2.8320
5	34 wks gest	6.9	5.7	1.2776
6	35 wks gest	8.1	4.2	1.1234
9	2 days old	3.8	3.7	1.2776
11	2 wks old	6.4	2.2	1.0930
		3.8	3.1	1.2014
16	1 mo, 23 days old	N/A	4.6	N/A
		N/A	7.2	N/A
18	2 mo, 9 days old	N/A	6.8	N/A
21	11 mo old	4.2	4.1	1.2511
22	12 mo old	16.2	3.5	0.3324

[a]Load and displacement instrumentation accuracy is 0.02% and 1.0×10^{-4}, respectively.

[b]Values not reported (indicated by N/A) were due to problems with displacement measurements.

Wks, weeks; gest, gestation; mo, month.

rameter that was sensitive to strain rate ($p = 0.035$), increasing with strain rate (Table 3).

Cranial Suture

All cranial suture data is provided in Table 2. Using a two-way ANOVA we found no significant effect of donor age or strain rate on the elastic modulus, ultimate stress, or ultimate strain of pediatric suture. However, modulus was significantly influenced by the interaction of donor age and strain rate ($p = 0.047$), such that the modulus of specimens from older donors tended to increase with strain rate while the modulus of specimens from younger donors tended to decrease with rate (Table 3).

Cranial Bone versus Cranial Suture

Because donor age and location of cranial bone were found to have a significant effect on bending modulus and ultimate stress, we focused our comparison of bone and suture properties on data obtained only from the parietal region and from subjects <1 month old ($n_{bone} = 8$, $n_{suture} = 9$). For this restricted data set, the modulus of parietal bone (315.8 ± 104.9 MPa, mean ± SE) was found to be significantly ($p = 0.011$, Fig. 5) stiffer than suture (7.6 ± 1.4 MPa). Ultimate stress of parietal bone (23.1 ± 9.4 MPa) was higher than suture (4.4 ± 0.5 MPa), but the power was not sufficient to reach significance ($p = 0.053$, power = 65%). Because none of the parameters (donor age, location, and strain rate) had significant effect on ultimate strain, we used the cranial bone and suture data from all donor ages and cranial locations provided in Tables 1 and 2 to evaluate ultimate strain, combining parietal and occipital tissue into the bone dataset. Cranial suture had a significantly ($p < 0.0001$) higher ultimate strain ($n = 9$, 1.460 ± 0.421 mm/mm) than cranial bone ($n = 46$, 0.043 ± 0.006 mm/mm).

DISCUSSION

This study provides much needed data regarding the material properties of human pediatric cranial bone and suture at rates of impact similar to those seen in low height falls. No study currently exists in the literature that has investigated the material properties of human pediatric cranial suture. Additionally, although there have been previous studies on pediatric cranial bone (Margulies and Thibault, 2000; McPherson and Kriewall, 1980a), they have been at extremely low rates relevant for studying vaginal delivery and may not be applicable

Table 3. Factors that Significantly Affect the Material Properties[a] of Infant Cranial Bone and Suture

Factor	*Bone*			*Suture*[b]		
Age	E	σ_{ult}	—	—	—	—
Strain rate	—	—	ε_{ult}	—	—	—
Location	E	σ_{ult}	—		n/a	
Age × strain rate	—	—	—	E	—	—
Age × location	—	—	—		n/a	
Rate × location	—	—	—		n/a	
Age × rate × location	—	σ_{ult}	—		n/a	

[a]Material properties: E, elastic modulus; σ_{ult}, ultimate stress; ε_{ult}, ultimate strain.

[b]Location is not applicable, because only coronal suture samples were obtained.

—, the material property is not affected by this factor.

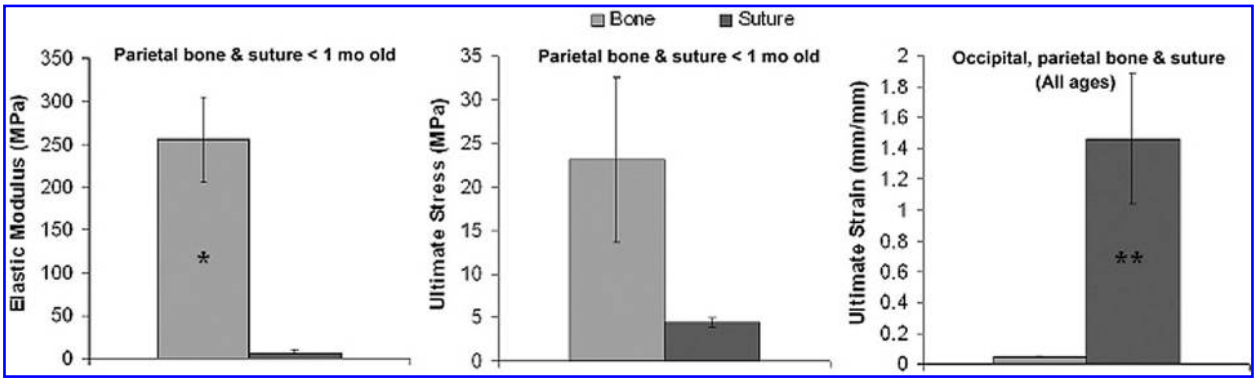

FIG. 5. Comparison of material properties of cranial bone to cranial suture. Significant differences were found for elastic modulus (*$p = 0.011$) and ultimate strain (**$p < 0.0001$), but did not reach significance for ultimate stress ($p < 0.053$). Due to age and location restrictions, the decreased sample size may not have been large enough to produce sufficient power for ultimate stress analyses (power = 65%).

for use at higher rates associated with accidental and inflicted impacts.

For donors between 21 weeks gestation and 13 months old, both bending modulus and ultimate stress significantly increase with the age of the donor. Previous studies on pediatric cranial bone (Margulies and Thibault, 2000; McPherson and Kriewall, 1980a) have found a similar influence of age on elastic modulus for donors ≤6 months old, regardless of test rate or fiber orientation included in the study. These data underscore the importance of investigating age-specific data to be used in age-specific computational models investigating pediatric head injury.

The parietal cranial bone was found to be significantly stiffer (461.1 ± 63.8 MPa) and have a higher ultimate stress (30.2 ± 4.8 MPa) than occipital cranial bone (329.0 ± 55.3 and 14.7 ± 2.1 MPa, respectively). Both elastic modulus and thickness contribute in a linear manner to the structural rigidity of the skull. However, the thickness of occipital bone was found to be approximately 1.5 times larger than parietal bone. Because the structural rigidity is proportional to thickness cubed, the rigidity of the occiput is 2.4 times that of the parietal bone. The larger structural rigidity and the lower ultimate stress of the occipital bone may imply that an impact to the occipital region of the skull will likely fracture and absorb energy before deformation whereas the parietal bone may be more likely to distribute the energy to surrounding sutures before distorting significantly and deforming the underlying brain. Because location plays a role in ultimate stress and bending modulus, the location of impact will influence the presence or absence of skull fracture seen in low height falls. Based on our material property data, skull should not be considered homogeneous when creating computational models to investigate impact events in pediatric head injury.

Contrary to our hypothesis, strain rate was *not* found to have a significant effect on the modulus and ultimate stress of cranial bone from donors ≤13 months old. This result is surprising given that Wood (1971) found strong rate dependence in human adult cortical skull. Previous pediatric cranial bone studies (Margulies and Thibault, 2000; McPherson and Kriewall, 1980a) did not have large enough sample sizes to make conclusions regarding human pediatric rate dependence. In a meta-analysis, we combined our data (restricted to <1 month old and parietal bone only) with published values for this age range in the literature (Fig. 6) to evaluate rate dependence of elastic modulus over 8 magnitudes of strain rate, and found no significant rate dependence in infant cranial bone.

Previous studies show that fiber orientation of immature cranial bone greatly affects the material properties. McPherson and Kriewall (1980a) analyzed specimens with fiber orientations both perpendicular and parallel to the long axis of their specimens. They found that the elastic modulus was significantly higher for specimens with fiber orientations parallel to the long axis than those with fiber orientations perpendicular to the long axis. McPherson and Kriewall (1980a,b, 1981) concluded from their series of studies that differences in material properties between pediatric and adult skull are most likely due to structural changes rather than material changes.

The fiber pattern of immature cranial bone emanates radially from ossification centers of each plate and is easily seen by the naked eye. Due to the difficulty of obtaining human samples, our study focused the investigation on testing the material properties in only one fiber orientation and specimens were excised such that fiber orientation was perpendicular to the long axis of the specimen. In this fiber orientation, we find no significant difference in elastic modulus (parietal bone, <1 month old)

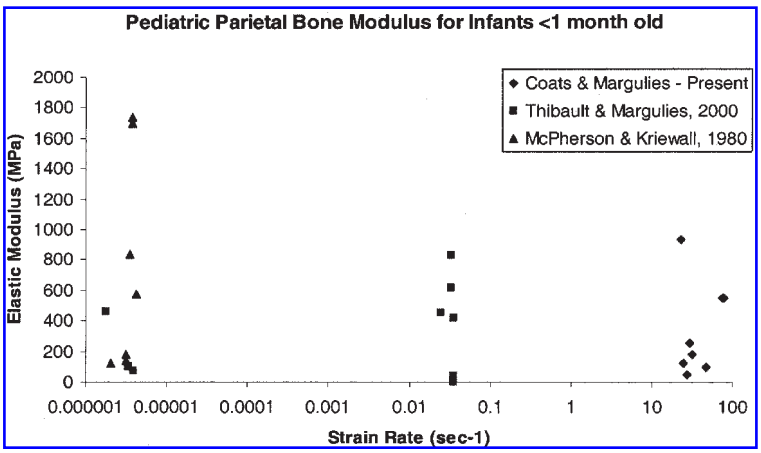

FIG. 6. Comparison of elastic modulus of cranial bone with values reported in the literature. To eliminate affects due to donor age or location, data from the present data set was restricted to only parietal bone and subjects <1 month old. Statistical analysis of the present study combined with values in the literature found no significant strain rate dependence over the broad range of rates tested. Note that the logarithmic scale is used for the *x*-axis.

to that reported by McPherson and Kriewall in specimens with the same fiber orientation ($p = 0.21$).

In contrast to pediatric skull, investigations of adult skull (a highly rate-dependent material) have found no visual pattern of fiber orientation (Dempster, 1967) and testing orientation of adult skull has no significant effect on the material properties (McElhaney et al., 1970; Wood, 1971).

Thus, we speculate that the difference between the rate dependence of pediatric and adult skull may be due to structural changes; specifically, the fiber orientation of the bone. Lynch et al. (2003) investigated the relation between rate dependence and fiber orientation in the tendon, another strongly fiber-oriented tissue. They report a strong rate dependence on tissue tested in tension in one fiber orientation, but no rate dependence when the tissue is tested in a fiber orientation perpendicular from the original configuration. We propose that, while no rate dependence was found in our meta-analysis of samples oriented perpendicularly to the fiber direction, there remains a possibility that future tests in a configuration parallel to the fibers may show rate dependence.

None of the material properties of cranial suture were affected by age or strain rate. It is important to note that sample size of cranial suture was small due to the fragility of the tissue. Specifically, samples with a tear or separation from the attached cranial bone prior to testing were excluded from this study. Despite the small sample size, a power analysis indicated that there was significant power for analysis (>94%) to evaluate rate and donor age dependence of suture tensile properties. Our analysis indicated that the interaction of donor age with strain rate did seem to have an effect on elastic modulus ($p = 0.0465$) implying that the effect of strain rate on elastic modulus changes with donor age, further emphasizing the need for more age related material property data. While the present study did not find this age-rate interaction to influence ultimate stress and strain, this could be due to testing a bone-suture-bone segment instead of suture alone. Due to the much larger elastic modulus of cranial bone than suture, the elastic moduli measured during tensile tests of bone-suture segments can be attributed mainly to the elastic modulus of the suture material alone. However, failure of the bone-suture-bone specimens consistently occurred at the bone-suture junction. From this it is reasonable to conclude that the measured ultimate stress and ultimate strain is more accurately the stress and strain of the suture material at the time when the junction between suture and bone fails. Because there was no visible damage to the suture material following each test, it is likely that the ultimate stress and ultimate strain of suture are higher than the values reported here.

There are no previous studies reporting the material properties of human pediatric cranial suture. Margulies and Thibault (2000) measured the material properties of immature (3–5 days old) porcine suture in tension and three-point bending. They reported the elastic modulus of suture was 171.5 MPa in tension (4.23×10^{-5} m/sec) and 194.2 MPa (4.23×10^{-5} m/sec) to 610.3 MPa (4.23×10^{-2} m/sec) in three-point bending. These values for porcine suture are 22–80 times stiffer than those of human pediatric suture, indicating that newborn porcine suture is not an appropriate model for human infant (<13 months old) pediatric suture.

Jaslow (1990) investigated the effect of cranial sutures on energy absorption during head impact of adult goats.

He reports that adult sutures absorbed 16–100% more energy per unit volume during impact loading than bone, highlighting the important role suture likely plays in the response to impact. In previous head injury computational models (Klinich et al., 2002; Lapeer and Prager, 2001), suture was assumed to have material properties similar to that of dura mater. McElhaney reported the elastic modulus of dura mater to be 31.5 MPa, four times stiffer than our measured modulus of pediatric suture (7.6 MPa). Because the measured modulus of human pediatric suture is lower than these estimated values, the pediatric skull would deform more during impact than previously thought.

Based on the material properties of suture in this dataset, a simple analysis was made to determine the possible deformation of suture as a result of increased intracranial pressure (ICP) seen following head trauma. The pediatric skull was idealized as two cranial bone hemispherical shells joined by a single sagittal suture. Using the elastic modulus values from our study, an increase in internal pressure from 10 mm Hg (normal infant ICP) to 50 mm Hg (infants with severe head trauma) (Barlow and Minns, 1999) increased stress in the suture by 5.33 kPa, elongating the suture only 0.03–0.14%. Even if the entire skull case was assumed to be composed of suture, the total volume change of the skull case would be 0.01–1.1%. This first-order analysis implies that an increase of ICP of 40 mm Hg in an infant deforms the suture only a minimal amount.

When comparing bone to suture, the dataset was restricted to parietal bone from subjects < 1 month old because donor age and location significantly influenced the material properties. Statistical analysis of the smaller data set found parietal bone to be more than 35 times stiffer than suture. Moreover, suture experienced strains over 100% before failing, 30 times more than cranial bone. Although the ultimate stress of parietal bone (23.1 ± 9.4 MPa) was larger than that of cranial suture (4.4 ± 0.5 MPa), more data is needed because this analysis lacked sufficient power (power = 65%) for significance in the reduced dataset. Taken together, these data supports the conceptual model of the pediatric skull as composed of bony plates connected by thin, weak extensible junctions.

In adults, cranial bone and suture have similar properties and the adult calveria deforms very little prior to fracture (Jaslow, 1990; McElhaney et al., 1970). In contrast, pediatric cranial bone is 35 times stiffer than pediatric cranial suture. In addition, pediatric cranial suture deforms 30 times more before failure than pediatric cranial bone and 243 times more than adult cranial bone (Wood, 1971). The large strains in the pediatric bone and suture result in a skullcase that can undergo dramatic shape changes before fracture, potentially causing substantial deformation in the brain. The sizeable difference between pediatric bone and suture material properties also underscores the crucial role that sutures play in the unique response of the pediatric head to impact in low height falls.

In conclusion, this study is the first to report human infant cranial bone and suture material properties over a broad range of strain rates. First, we found that strain rate did not have a significant effect on the material properties of cranial bone and suture, and we propose that the role of fiber orientation should be investigated further. Second, we found that donor age had the largest influence on the elastic modulus and ultimate stress of cranial bone, further emphasizing the need for age-specific data and computational models. Third, we found that cranial bone was 35 times stiffer than suture, and that suture tolerated over 100% strain before the bone-suture junction failed. Taken together, these findings illustrate the unique material properties of human pediatric skull and suture, furthering our understanding of the pediatric skull and suture response to impact, and contributing to the development of more accurate computational models needed to investigate accidental and inflicted pediatric head injury.

ACKNOWLEDGMENTS

We would like to thank Dr. Alex Radin for his insight on material property testing, as well as the CDC and NIH for their support of this work: CDC-NCIPC R49-CE000411-01 (to B.C.) and NIH-R01-NS39679 (to S.S.M.).

REFERENCES

BARLOW, K.M., and MINNS, R.A. (1999). The relation between intracranial pressure and outcome in non-accidental head injury. Dev. Med. Child Neurol. **41,** 220–225.

CHADWICK, D.L., CHIN, S., SALERNO, C., et al. (1991). Deaths from falls in children: how far is fatal? J. Trauma **31,** 1353–1355.

COATS, B., and MARGULIES, S.S. (2005). High rate material properties of infant cranial bone and suture. ASME Summer Bioengineering Conference: Vail, CO.

DEMPSTER, W.T. (1967). Correlation of types of cortical grain structure with architectural features of the human skull. Am. J. Anat. **120,** 7–32.

JASLOW, C.R. (1990). Mechanical properties of cranial sutures. J. Biomech. **23,** 313–321.

KLINICH, K., HULBERT, G., and SCHNEIDER, L. (2002). Estimating infant head injury criteria and impact response

using crash reconstruction and finite element modeling. Stapp Car Crash J. **46,** 165–194.

LANE, W., RUBIN, D., MONTEITH, R., et al. (2002). Racial differences in the evaluation of pediatric fractures for physical abuse. JAMA **288,** 1603–1609.

LANGLOIS, J., RUTLAND-BROWN, W., and THOMAS, K. (2004). Traumatic brain injury in the united states: emergency department visits, hospitalizations, and deaths. Centers for Disease Control and Prevention, National Center for Injury Prevention and Control: Atlanta.

LAPEER, R.J., and PRAGER, R.W. (2001). Fetal head moulding: finite element analysis of a fetal skull subjected to uterine pressures during the first stage of labour. J. Biomech. **34,** 1125–1133.

LYNCH, H.A., JOHANNESSEN, W., WU, J.P., et al. (2003). Effect of fiber orientation and strain rate on the nonlinear uniaxial tensile material properties of tendon. J. Biomech. Eng. **125,** 726–731.

MARGULIES, S.S., and THIBAULT, K.L. (2000). Infant skull and suture properties: measurements and implications for mechanisms of pediatric brain injury. J. Biomech. Eng. **122,** 364–371.

McELHANEY, J.H., FOGLE, J.L., MELVIN, J.W., et al. (1970). Mechanical properties of cranial bone. J. Biomech. **3,** 495–511.

McPHERSON, G., and KRIEWALL, T. (1980a). The elastic modulus of fetal cranial bone: a first step toward understanding of the biomechanics of fetal head molding. J. Biomech. **13,** 9–16.

McPHERSON, G.K., and KRIEWALL, T.J. (1980b). Fetal head molding: an investigation utilizing a finite element model of the fetal parietal bone. J. Biomech. **13,** 17–26.

McPHERSON, G.K., and KRIEWALL, T.J. (1981). Bending properties and ash content of fetal cranial bone. J. Biomech. **14,** 73–39.

TARANTINO, C.A., DOWD, M.D., and MURDOCK, T.C. (1999). Short vertical falls in infants. Pediatr. Emerg. Care **15,** 5–8.

TIMOSHENKO, S., and GOODIER, J. (1970). *Theory of Elasticity.* McGraw-Hill: New York.

WEBER, W. (1984). [Experimental studies of skull fractures in infants]. Z. Rechtsmed. **92,** 87–94.

WEBER, W. (1985). [Biomechanical fragility of the infant skull] german. Z. Rechtsmed. **94,** 93–101.

WILLIAMS, R.A. (1991). Injuries in infants and small children resulting from witnessed and corroborated free falls. J. Trauma **31,** 1350–1352.

WOOD, J.L. (1971). Dynamic response of human cranial bone. J. Biomech. **4,** 1–12.

Address reprint requests to:
Susan S. Margulies, Ph.D.
Department of Bioengineering
University of Pennsylvania
3320 Smith Walk, Ste. 120
Philadelphia, PA 19104-6392

E-mail: margulie@seas.upenn.edu

This article has been cited by:

1. Charles Davis, Claes G. K. Lauritzen. 2010. The Biomechanical Characteristics of Cranial Sutures Are Altered by Spring Cranioplasty Forces. *Plastic and Reconstructive Surgery* **125**:4, 1111-1118. [CrossRef]
2. Charles Davis, Per Windh, Claes G. K. Lauritzen. 2010. Cranial Bone and Suture Strains Incident to Spring-Assisted Cranioplasty. *Plastic and Reconstructive Surgery* **125**:4, 1104-1110. [CrossRef]
3. Charles Davis, Per Windh, Claes G. K. Lauritzen. 2010. Adaptation of the cranium to spring cranioplasty forces. *Child's Nervous System* **26**:3, 367-371. [CrossRef]
4. Angela K. Thompson, Gina Bertocci, Mary Clyde Pierce. 2009. Assessment of Head Injury Risk Associated With Feet-First Free Falls in 12-Month-Old Children Using an Anthropomorphic Test Device. *The Journal of Trauma: Injury, Infection, and Critical Care* **66**:4, 1019-1029. [CrossRef]
5. Timothy G. Baumer, Brian J. Powell, Todd W. Fenton, Roger C. Haut. 2009. Age Dependent Mechanical Properties of the Infant Porcine Parietal Bone and a Correlation to the Human. *Journal of Biomechanical Engineering* **131**:11, 111006. [CrossRef]
6. Brittany Coats, Susan S. Margulies. 2008. Potential for head injuries in infants from low-height falls. *Journal of Neurosurgery: Pediatrics* **2**:5, 321-330. [CrossRef]
7. Mary Clyde Pierce, Gina Bertocci. 2008. Injury Biomechanics and Child Abuse. *Annual Review of Biomedical Engineering* **10**:1, 85-106. [CrossRef]